

PSFC/RR-97-7

**Feasibility Study of an Iterative Finite  
Difference Approach to Kinetic Modeling  
of Neutral Particles in Edge Plasmas**

M L Adams<sup>1</sup>, S I Krasheninnikov<sup>2</sup>,  
O V Batishchev<sup>3</sup>

April 1997

Plasma Science and Fusion Center  
Massachusetts Institute of Technology  
Cambridge, Massachusetts 02139 USA

<sup>1</sup>Permanent address: Lake George NY 12845 USA

<sup>2</sup>Also at Kurchatov Institute of Atomic Energy, Moscow 123098 Russia

<sup>3</sup>Permanent address: Keldysh Institute for Applied Mathematics, Moscow 125047 Russia

This work was supported by the US Department of Energy, Grant No. DE-FG02-91ER54109.  
Reproduction, translation, publication, use, and disposal, in whole or in part, by or for the US  
Government is permitted.

## Abstract

Numerical stability describes the difference between a computational solution and an exact solution as the number of iterations increases — in stable simulations the computational solution will approach the exact solution. Discretisation of the kinetic equation using a Krook collision operator, by a common finite difference method, is found to have a time step stability limit much less than the mean free path ( $\Delta t v_{th} \ll \lambda$ ). Due to high neutral density in the divertor region, hence low mean free path, this stability limit prohibits feasible numerical simulations. However, formulating an integral solution of the Krook equation before discretisation is found to alleviate the time step stability limit ( $\Delta t \geq 0$ ). As the Krook equation is highly nonlinear, and a detailed error analysis is beyond the scope of this initial study, we gain confidence in our results through a series of plane Couette flow simulations. Errors are found to be minimal and further study of kinetic neutral modeling in edge plasmas is warranted.

# 1 Introduction

At the turn of the decade, Stangeby and M<sup>c</sup>Cracken [1] conjectured that reducing the high divertor target plate incident heat flux as “a major engineering obstacle to the successful operation of fusion reactors”. In 1995, Post [2] presented a review of several atomic processes that would, in principle, distribute the heat flux over reactor regions other than the divertor target plate. These processes include: 1) radiation losses through bremsstrahlung from the central plasma; 2) impurity radiation losses from the plasma edge and divertor plasma; 3) charge exchange radiation losses from the scrape-off layer (SOL) and divertor plasma; and 4) hydrogen radiation losses from the SOL and divertor plasma. Today, current research [3] has pointed toward the importance of neutral-neutral collisions in any divertor study and the demand for an efficient code allowing for such interactions, along with plasma-neutral interactions, is on the rise.

Neutral particle densities in edge plasmas vary over several orders of magnitude. In the divertor region neutral density may increase to the level where the neutral-neutral interaction mean free path is of the order of millimeters, and thus becomes a dominant process. Demonstrated in the next section, typical finite difference numerical kinetic modeling of neutrals is hindered by a time step limit less than the mean free path. Current codes have focused on other methods of solution. Pragmatic approaches include linear Monte-Carlo and finite difference fluid models. Unfortunately, for regimes of most interest to divertor operation, plasma and neutral gas parameters in the SOL vary enough to prohibit either method from providing an entirely satisfactory description of neutral transport. Addressing this dilemma, we present the following feasibility study of an iterative finite difference approach to kinetic modeling of neutral particles in edge plasmas.

This paper proceeds as follows: *Section 2* assumes that numerical stability is the necessary and sufficient condition for convergence (correct for any well-posed problem with consistent discretisation) and demonstrates a method for obtaining global stability; *Section 3* defines plane Couette flow and presents an exact Navier-Stokes solution; *Section 4* includes 1D2V plane Couette flow simulation results; *Section 5* extends the 1D2V simulation to 2D2V; *Section 6* investigates a range of Knudsen numbers in 1D2V and flow around an obstacle in 2D2V; and *Section 7* concludes the feasibility study with suggestions for pertinent areas of future research.

## 2 Theoretical Background

We begin by introducing an equation that adequately describes the behavior of neutral particles in edge plasmas. Direct discretisation of the governing equation is found to yield unstable numerical results. A general method is found, extrapolated from the work of Shakhov [4], for formulating an integral equation before discretisation which yields stable numerical results.

### 2.1 Kinetic Equation with Krook Collision Operator

To describe the behavior of neutral particles in edge plasmas we start with the Boltzmann equation. After replacing the full collision integral with a model term (introduced simultaneously by the Bhatnagar, Gross, and Krook (BGK) and Welander) and neglecting external forces we may write:

$$\frac{\partial f}{\partial t} + \vec{c} \cdot \frac{\partial f}{\partial \vec{r}} = -\frac{(f - f^M)}{\tau}, \quad (1)$$

where  $\vec{r}$ ,  $\vec{c}$ , and  $\tau$  represent spatial coordinate, molecular velocity, and collision interval time respectively;  $f^M$  is the Maxwellian velocity-distribution function containing the following self-consistent terms describing macroscopic properties of a gas: number density

$$n(\vec{r}) = \int f(\vec{r}, \vec{c}) d^3 \vec{c}, \quad (2)$$

mean molecular velocity

$$\vec{c}_0(\vec{r}) = \frac{\int f(\vec{r}, \vec{c}) \vec{c} d^3 \vec{c}}{n(\vec{r})}, \quad (3)$$

and temperature

$$T(\vec{r}) = \frac{\int f(\vec{r}, \vec{c}) m (\vec{c} - \vec{c}_0(\vec{r}))^2 d^3 \vec{c}}{3n(\vec{r})}, \quad (4)$$

where  $m$  is the molecular mass. Equation 1 is commonly referred to as the Krook equation. [5, 6, 7]

Numerical stability describes the difference between a computational solution and an exact solution as the number of iterations increases. If a numerical scheme is stable the computational solution will approach the exact solution; in an unstable numerical scheme the difference between computational solution and exact solution will increase. We examine the stability of Eq. 1 by using an implicit Euler method for discretisation. Following application of a mobile operator ( $\frac{d}{dt} = \frac{\partial}{\partial t} + \vec{c} \cdot \frac{\partial}{\partial \vec{r}}$ ) to the left-hand-side (LHS), discretisation, and a little algebra the Krook equation becomes:

$$f_b = \frac{1}{1 + \frac{\Delta t}{\tau_b}} (f_a + \frac{\Delta t}{\tau_b} f_b^M), \quad (5)$$

where  $\vec{b} = \vec{a} + \vec{c} \Delta t$ . For numerical stability this equation requires  $\frac{\Delta t}{\tau_b} \ll 1$  or  $\Delta t v_{th} \ll \lambda$ , where  $v_{th}$  is the thermal velocity and  $\lambda$  is the mean free path. Actually, since this equation is stable in the limit  $\Delta t \rightarrow 0$ , it is numerically unstable.

## 2.2 Integral Krook Equation

Generalizing the work of Shakhov, an operator is chosen to transform a governing equation into a first-order linear differential equation and an exponential antiderivative is chosen to yield a solution. With the mobile operator and  $\exp[\int_0^t \frac{1}{\tau} dt']$  for our exponential antiderivative, we may write the following integral form of Krook's equation:

$$f(t) = e^{-\int_0^t \frac{1}{\tau} dt'} f(0) + \int_0^t \frac{1}{\tau} e^{-\int_{t'}^t \frac{1}{\tau} dt''} f^M dt'. \quad (6)$$

Discretisation of Eq. 6 is achieved through the use of a linear Taylor series expansion for the Maxwellian velocity-distribution function and definition of a local mean collision interval ( $\bar{\tau}^{-1} = \frac{\tau_a^{-1} + \tau_b^{-1}}{2}$ ). After applying the fundamental theorem of calculus and performing some trivial algebra, the integral Krook equation becomes:

$$f_b = f_a e^{-\frac{\Delta t}{\bar{\tau}}} + f_b^M [1 - e^{-\frac{\Delta t}{\bar{\tau}}}] + \frac{\Delta f^M}{\Delta t} \{ \Delta t e^{-\frac{\Delta t}{\bar{\tau}}} + \bar{\tau} [1 - e^{-\frac{\Delta t}{\bar{\tau}}}] \}, \quad (7)$$

where  $\bar{b} = \bar{c}\Delta t + \bar{a}$ . This equation is numerically stable for  $\frac{\Delta t}{\bar{\tau}} \geq 0$ . In the continuum limit, as  $\frac{\Delta t}{\bar{\tau}}$  goes to infinity,  $f_b$  approaches  $f_b^M$ ; in the rare-gas limit, as  $\frac{\Delta t}{\bar{\tau}}$  goes to zero, we see that  $f_b$  approaches  $f_a$ . We have transformed an unstable computational scheme into a stable scheme with the added benefit of removing any relation between mesh spacing and mean free path.

### 3 Plane Couette Flow and Navier-Stokes Solution

To test a new solution technique for kinetic neutral gas phenomenon, the analysis of plane Couette flow is a natural consideration. Plane Couette flow, [8, 9, 10, 11] within the class of parallel-plate flow problems, is distinguished by: 1) a fixed separation distance  $L$ ; 2) equal and constant plate temperatures ( $T|_{\text{lower plate}} = T|_{\text{upper plate}} = T_p$ ); and 3) a constant relative plate velocity [In this paper, the upper plate is fixed ( $V|_{\text{upper plate}} = 0$ ) and the lower plate is set in constant subsonic motion ( $V|_{\text{lower plate}} = V_p$ ;  $V_p \ll v_{th}$ ).]. Refer to Fig. 1 for visual clarification.

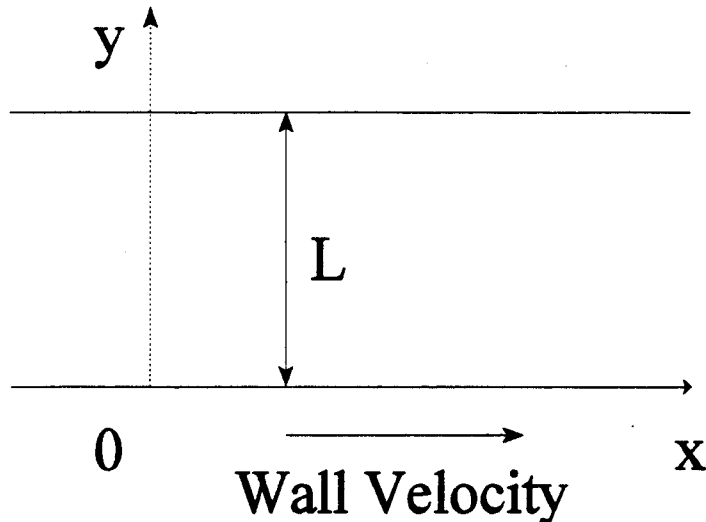


Figure 1: Plane Couette Flow

In the continuum limit an exact solution for plane Couette flow may be found by using the Navier-Stokes equation. As neutral gas increases in density, neutral-neutral collisions become more frequent, and the mean free path decreases. Relating the continuum limit to gas parameters, we write for the mean free path:

$$\frac{\lambda_r}{L_r} = \text{Kn} = \frac{\bar{c}_0}{\text{Re}}, \quad (8)$$

where  $\text{Kn}$  is the Knudsen number, a dimensionless parameter defined by the LHS of Eq. 8;  $\text{Re}$  is the Reynold's number, a useful dimensionless parameter for most flow problems describing the ratio of inertia force to viscous force;  $\bar{c}_0$  is the average mean molecular velocity; and the subscript  $r$  denotes a reference value. To analyze plane Couette flow, and establish a relation to kinetic simulations in the continuum regime, we assign  $\text{Kn} = 0.01$  ( $L_r = L$ ) and assume laminar flow (low  $\text{Re}$ ).

Using the one-dimensional nature of the problem, assuming a negligible pressure gradient ( $n = T = \text{constant}$ ), and applying the boundary condition used to define relative parallel plate motion we write:

$$c_{x0} = V_p \left(1 - \frac{y}{L}\right); \quad (9)$$

$$c_{y0} = c_{z0} = 0; \quad (10)$$

$$n = n_r; \text{ and } T = T_p; \quad (11)$$

where  $n_r$  is a constant reference density. With  $V_p = 0.1v_{th}$ , the reader may note  $Re = 5$ , validating our assumption of laminar flow. The Navier-Stokes solution will be used to estimate the accuracy of our numerical simulations.

## 4 1D2V Simulation of Plane Couette Flow

In this section, our technique to alleviate a mesh spacing stability limit is applied to plane Couette flow in the continuum regime; results are then compared to the exact Navier-Stokes solution.

### 4.1 Governing Integral Equation Formulation

*Section 2* highlighted the potential of formulating an integral equation before discretisation; in theory, with any mesh spacing, the computational solution should approach the exact solution as the number of iterations increase. This approach is applied to plane Couette flow by first writing the Krook equation in an appropriate one-dimensional form and then establishing an associated dimensionless form.

In 1D2D the Krook equation reduces to:

$$c_{y0} \frac{\partial f}{\partial y} = -\frac{(f - f^M)}{\tau}. \quad (12)$$

Introducing the following dimensionless parameters:  $\hat{f} = f v_{th}^3$ ,  $\hat{f}^M = f^M v_{th}^3$ ,  $\hat{\tau} = \frac{\tau}{L}$ ,  $\hat{c} = \frac{c}{v_{th}}$ ,  $\hat{T} = \frac{T}{v_{th}^2}$ ,  $\hat{n} = \frac{n}{n_r}$ ,  $\hat{\tau} = \frac{\tau}{\tau_r}$ ,  $\hat{\lambda} = \frac{\lambda}{\lambda_r}$ , and  $v_{th}^2 = \frac{3}{2}T$ ; and recalling the following definitions:  $Kn = \frac{\lambda_r}{L_r}$  and  $\tau = \frac{\lambda}{v_{th}^2}$ ; allows us to write the following dimensionless form of Eq. 12:

$$\hat{c}_{y0} \frac{\partial \hat{f}}{\partial \hat{y}} = -\frac{L}{\hat{\tau} \tau_r v_{th}} (\hat{f} - \hat{f}^M) = -\frac{(\hat{f} - \hat{f}^M)}{Kn}. \quad (13)$$

For the remainder of the paper dimensionless parameters are used and the “hat” notation is dropped for simplification.

Choosing an appropriate operator and exponential antiderivative we formulate an integral equation. No operator is needed since Eq. 13 is already a first-order linear differential equation;  $\exp[\int_0^y \frac{1}{c_{y0} Kn} dy']$  is used for our exponential antiderivative. After applying some algebra and the fundamental theorem of calculus we may write:

$$f(y) = e^{-\int_0^y \frac{1}{c_{y0} Kn} dy'} f(0) + \int_0^y \frac{1}{c_{y0} Kn} e^{-\int_{y'}^y \frac{1}{c_{y0} Kn} dy''} f^M dy'. \quad (14)$$

Note the similarity between this equation to that of the general integral equation given in *Section 2*. The only difference lies in possible particle trajectories.

## 4.2 Discretisation

A computational solution for ideal comparison to the exact Navier-Stokes solution, suitable for a stability analysis, is constructed through minimal discretisation complexity. The average collision interval approximation is eliminated by using the fixed Knudsen number depicting laminar flow. After a Taylor series expansion of the Maxwellian velocity-distribution function, we write the following numerical approximation:

$$f_b = f_a e^{-\frac{\Delta y}{c_{y0} Kn}} + f_b [1 - e^{-\frac{\Delta y}{c_{y0} Kn}}] + \frac{\Delta f^M}{\Delta y} \{ \Delta y e^{-\frac{\Delta y}{c_{y0} Kn}} + c_{y0} Kn [1 - e^{-\frac{\Delta y}{c_{y0} Kn}}] \}, \quad (15)$$

where  $b = a + \Delta y$ . Although only one finite difference approximation was used, that associated with the Maxwellian velocity-distribution, this is still a highly nonlinear numerical equation. As an *a priori* error analysis of this equation would be another paper by itself, and definitely beyond the scope of this initial feasibility study, preparations will be made for an *a posteriori* error analysis.

Aside from the error ( $O(\Delta y)$ ) introduced by the Taylor series expansion of the Maxwellian velocity-distribution function, sources of numerical error include the integration process and machine accuracy. Integration errors are associated with: 1) method of numerical solution, 2) mesh spacing (number of nodes in velocity space), and 3) truncation of an infinite velocity space; machine accuracy will increase as the number of operations per iteration increases. In an effort to minimize the errors not associated with the Maxwellian velocity-distribution function, we have developed an algorithm that balances integration and machine accuracy factors. From the results of this algorithm: integration is performed with an upper approximation; a  $21 \times 21$  uniform velocity mesh is used (effects of variable velocity mesh spacing were not analyzed); and the velocity space domain is  $-5.5 \leq (c_x, c_y) \leq 5.5$ .

## 4.3 Qualitative Stability Analysis

Numerical simulations were performed with an increasing degree of nonlinearity. First simulation: all assumptions used in deriving the Navier-Stokes solution are used ( $n = T = 1.0; V_p = 0.1$ ). Second simulation: temperature is allowed to vary in the central flow region ( $n = 1.0; V_p = 0.1; T_p = 1.0$ ). Third simulation: full nonlinearity of the Maxwellian velocity-distribution is retained ( $V_p = 0.1; T_p = 1.0$ ). Results of these simulations are displayed in Figs. 2, 3, 4, and 5.

In the first simulation the error is not noticeable. In fact, the error is of order machine epsilon ( $2^{-53}$ ), defined as the greatest floating point number such that  $1 - \epsilon = 1$  is correct. This allows us to relate the errors associated with higher degrees of nonlinearity to the Maxwellian velocity-distribution function approximation. In the second simulation allowing the central temperature to vary is found to be destabilizing. Temperature variations introduce a noticeable effect on the velocity, however their respective magnitudes of error are consistent with their velocity ordering. In the third simulation, density variations in the central flow region and conservation of flux at the boundary are found to be stabilizing with respect to the velocity and destabilizing with respect to temperature. From these simulations we estimate the error introduced by a linear Taylor series expansion of the Maxwellian to be of the order  $10^{-1}\%$  for temperature,  $10^{-2}\%$  for density, and  $10^{-5}\%$  for velocity.



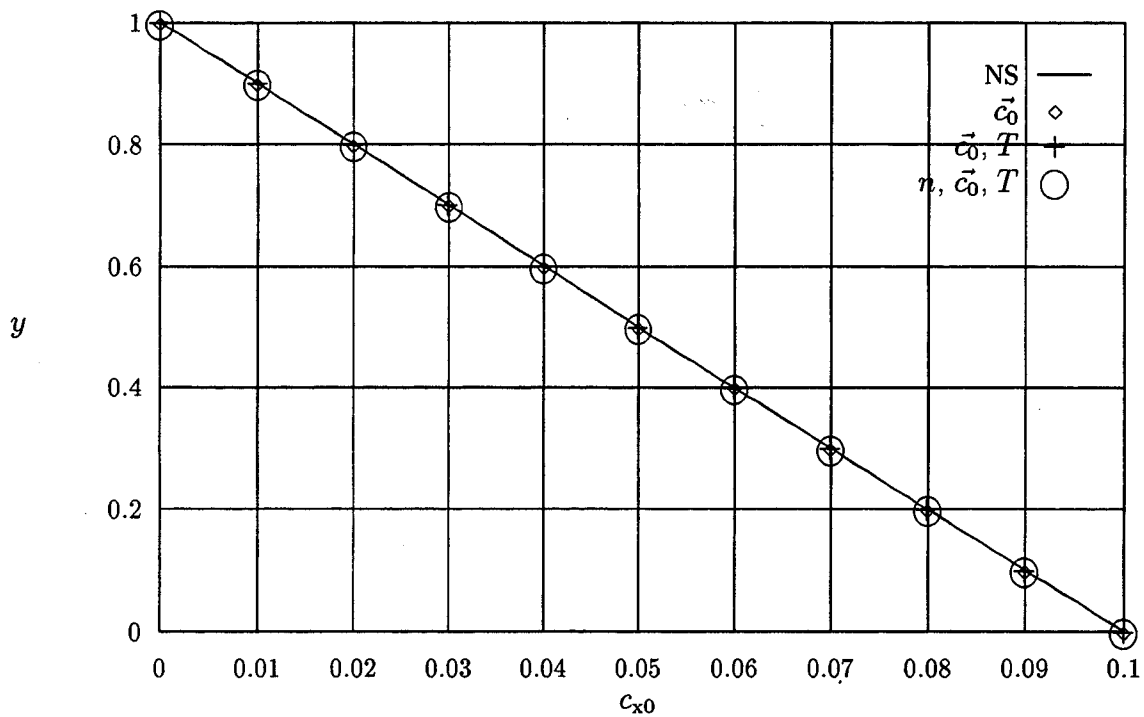


Figure 2: Mean Molecular Velocity in the  $x$ -Direction

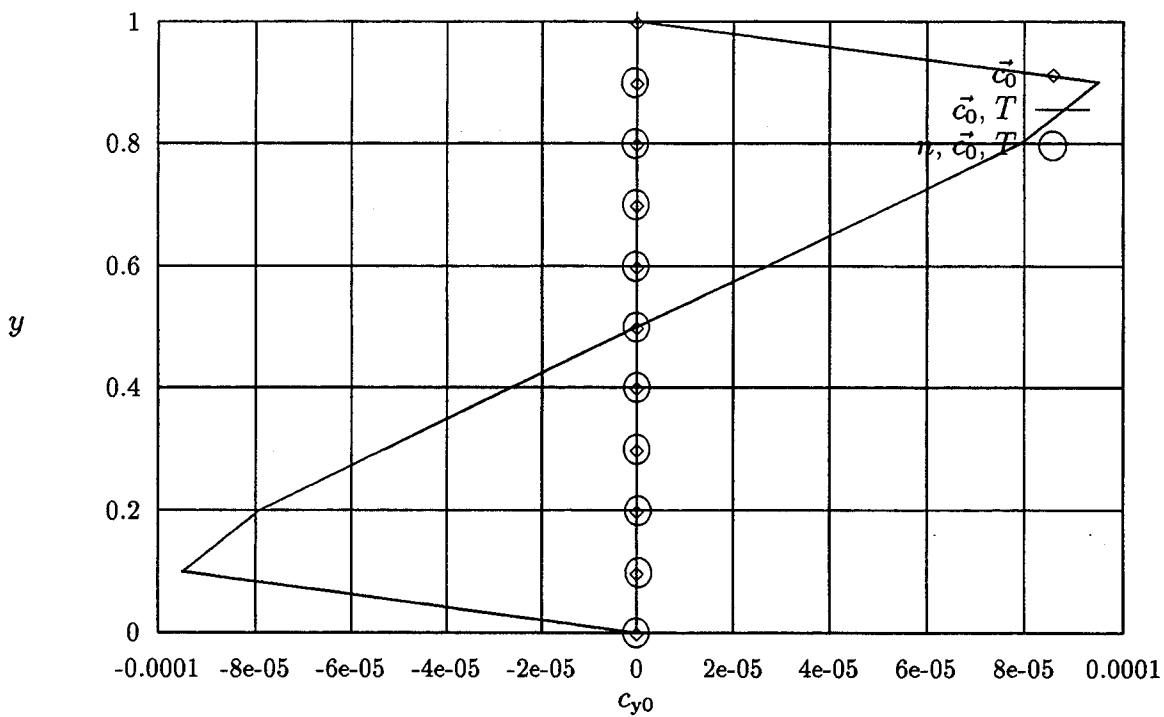


Figure 3: Mean Molecular Velocity in the  $y$ -Direction

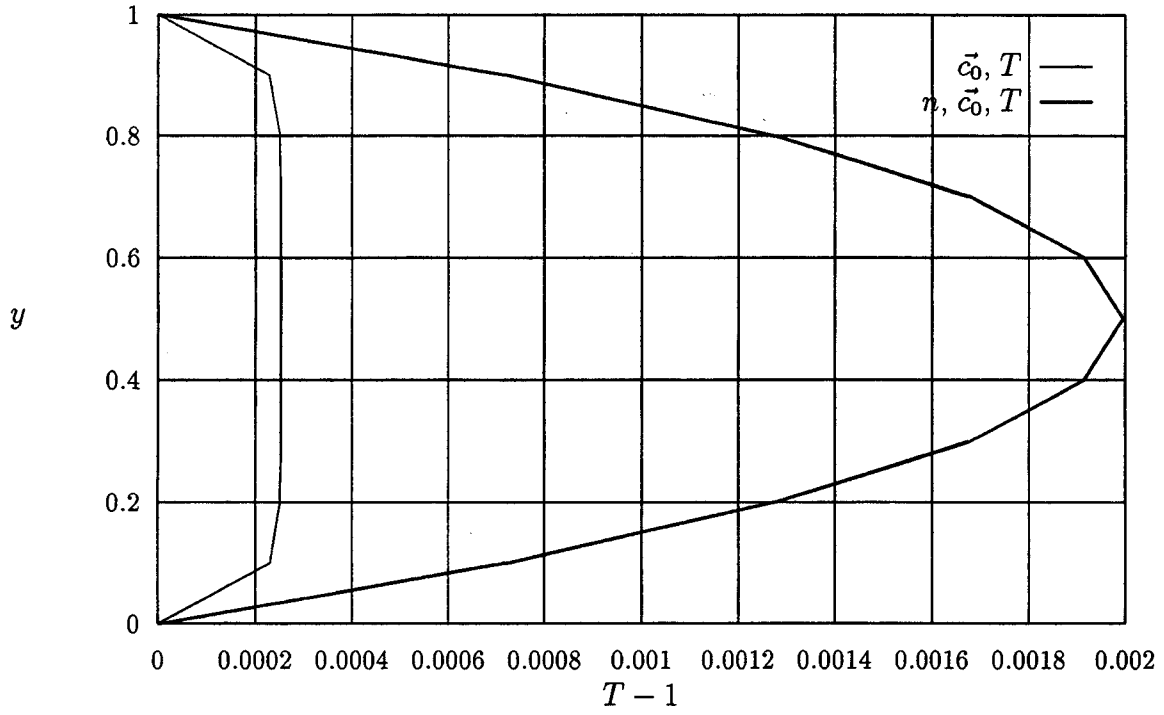


Figure 4: Temperature

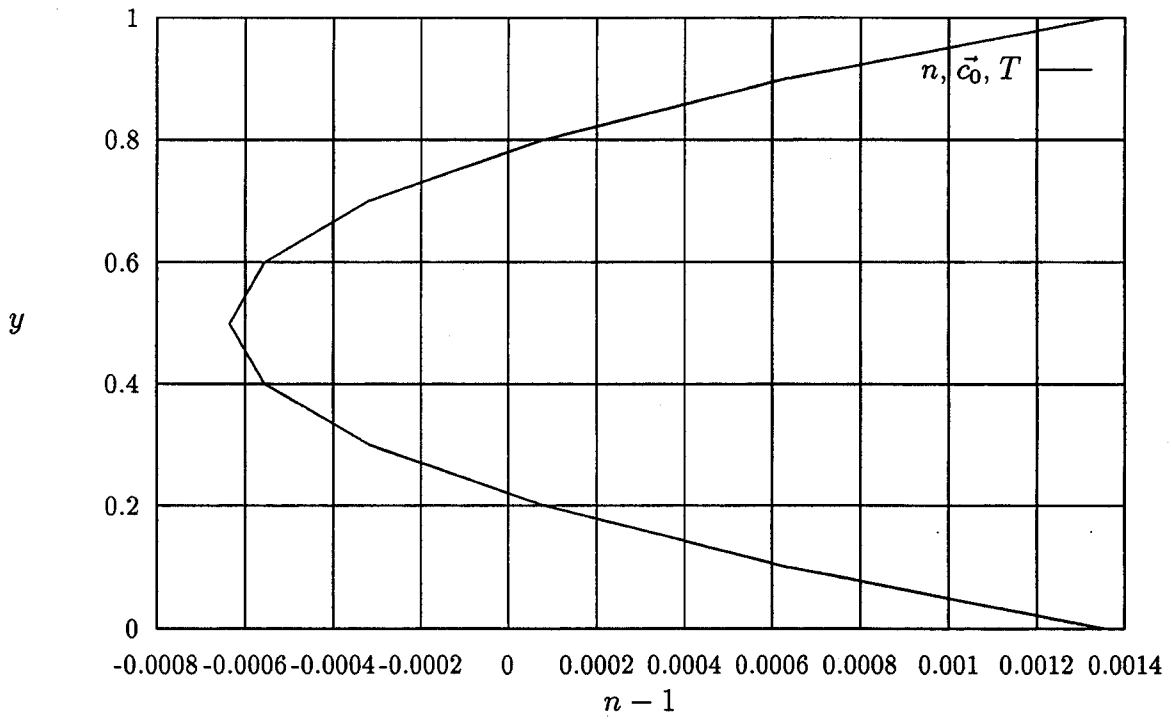


Figure 5: Density

## 5 2D2V Simulation of Plane Couette Flow

In this section, the one-dimensional analysis presented in *Section 4* is extended to two dimensions. This will require the use of an operator (unlike the 1D case) and a method for integrating along characteristic trajectories.

### 5.1 Formation of a Governing Integral Equation

Using the convective derivative, that part of the mobile operator dealing with spatial derivatives, for an operator allows us to reformulate the Krook equation for higher spatial dimensions as:

$$\vec{c} \cdot \vec{\nabla} f = -\frac{1}{Kn} (f - f^M). \quad (16)$$

The convective derivative describes the velocity along characteristic trajectories. In kinetic theory, since velocity and space are independent variables, we may describe the direction of trajectories by  $\frac{\vec{c}}{|\vec{c}|}$  and the velocity magnitude along the trajectory by  $|\vec{c}|$  (speed). After using these concepts Eq. 16 becomes:

$$|\vec{c}| \frac{df}{d\xi} = -\frac{1}{Kn} (f - f^M), \quad (17)$$

where  $\xi$  is the trajectory coordinate. This is a linear first-order differential equation along characteristic trajectories. Choosing our exponential antiderivative as  $\exp[\int_0^\xi \frac{1}{|\vec{c}|Kn} d\xi']$ , we integrate to obtain:

$$f(\xi) = e^{-\int_0^\xi \frac{1}{|\vec{c}|Kn} d\xi'} f(0) + \int_0^\xi \frac{1}{|\vec{c}|Kn} e^{-\int_{\xi'}^\xi \frac{1}{|\vec{c}|Kn} d\xi''} f^M d\xi' \quad (18)$$

Again, this equation is similar to the general governing integral equation given in *Section 2*.

### 5.2 Discretisation

Discretisation is complicated by the freedom of characteristic trajectories; it is common for trajectories to miss existing nodes. For extending our numerical analysis into 2D, we recall the successful factors of 1D and attempt to approximate the initial distribution function from a backward step along the characteristic curve. Figure 6 is included to clarify the value of  $f_a$  used in the following equation:

$$f_b = f_a e^{-\frac{\Delta\xi}{|\vec{c}|Kn}} + f_b^M [1 - e^{-\frac{\Delta\xi}{|\vec{c}|Kn}}] + \frac{\Delta f^M}{\Delta\xi} \{ \Delta\xi e^{-\frac{\Delta\xi}{|\vec{c}|Kn}} + |\vec{c}|Kn [1 - e^{-\frac{\Delta\xi}{|\vec{c}|Kn}}] \}. \quad (19)$$

An *a posteriori* error analysis may now focus on the difference between 1D and the 2D results, attributing deviations in space to the approximate initial distribution function.

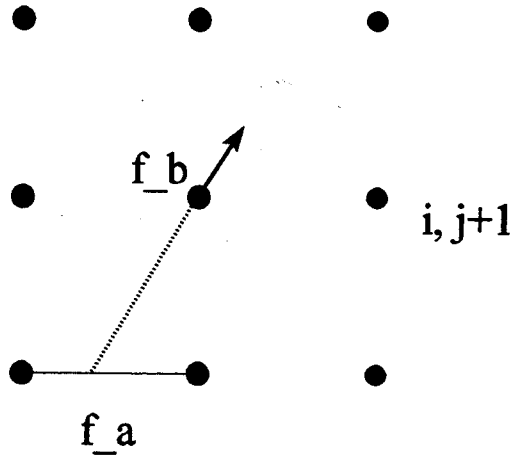


Figure 6: Method for Approximating the Initial Distribution Function

### 5.3 Self-Consistent 2D2V Couette Flow Simulation

Figures 7, 8, 9, and 10 present the 2D2V results obtained with full nonlinearity of the Maxwellian velocity-distribution function and periodic boundary condition. Negligible profile variation along the horizontal dimension validates the 2D2V results.

Effects of the  $f^M$  and  $f_a$  approximation were obtained in the continuum regime and should not be assumed to carry over to the rare-gas regime. Actually, error contributions are reversed for higher Knudsen numbers.

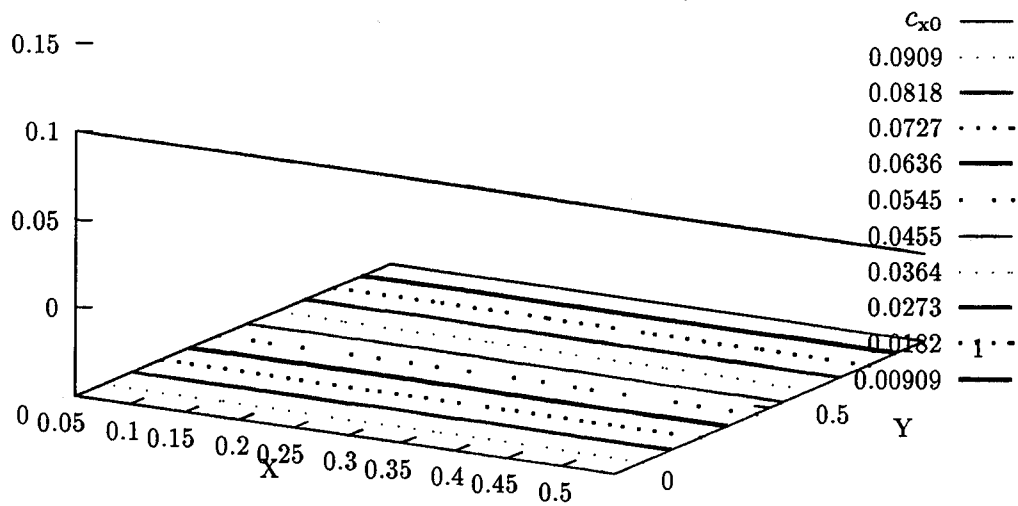


Figure 7: Mean Molecular Velocity in the  $x$ -Direction

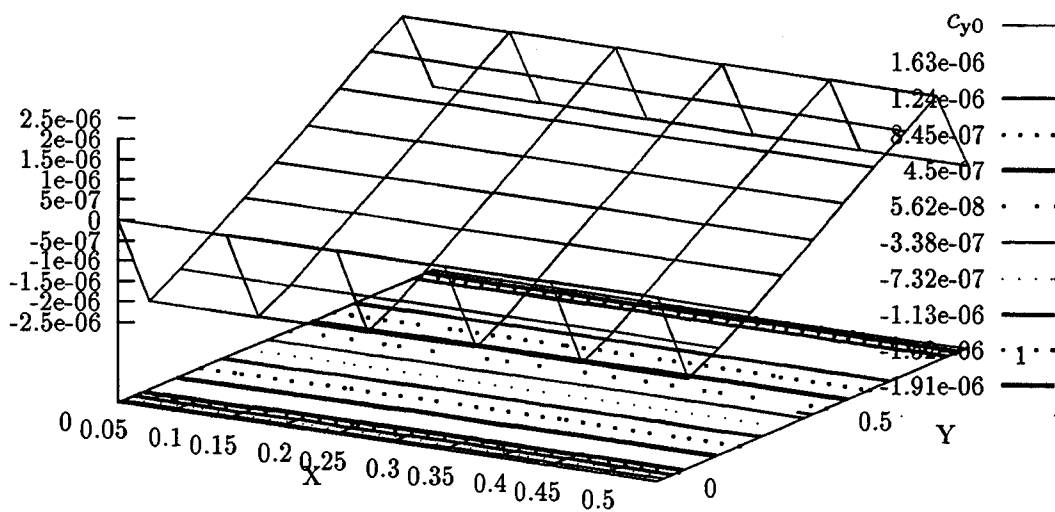


Figure 8: Mean Molecular Velocity in the  $y$ -Direction

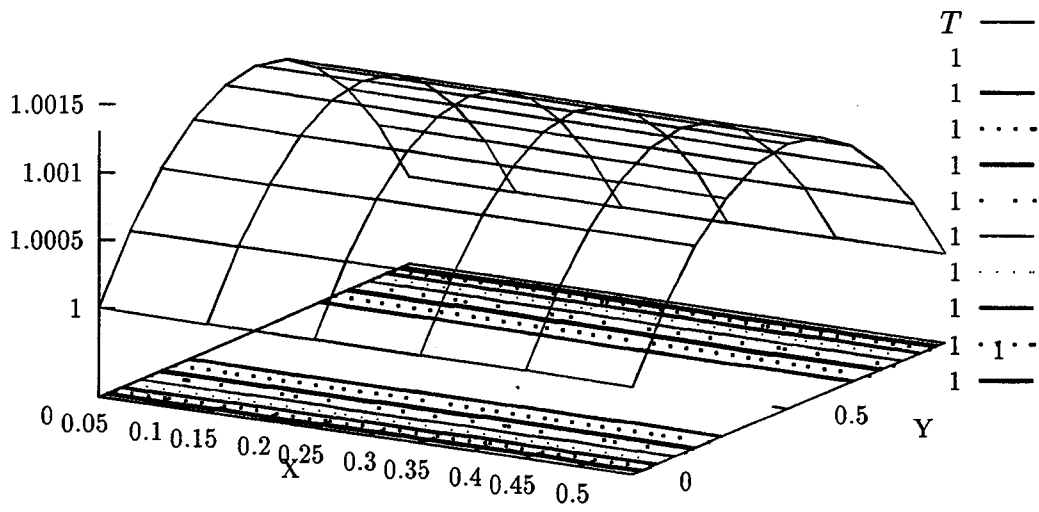


Figure 9: Temperature

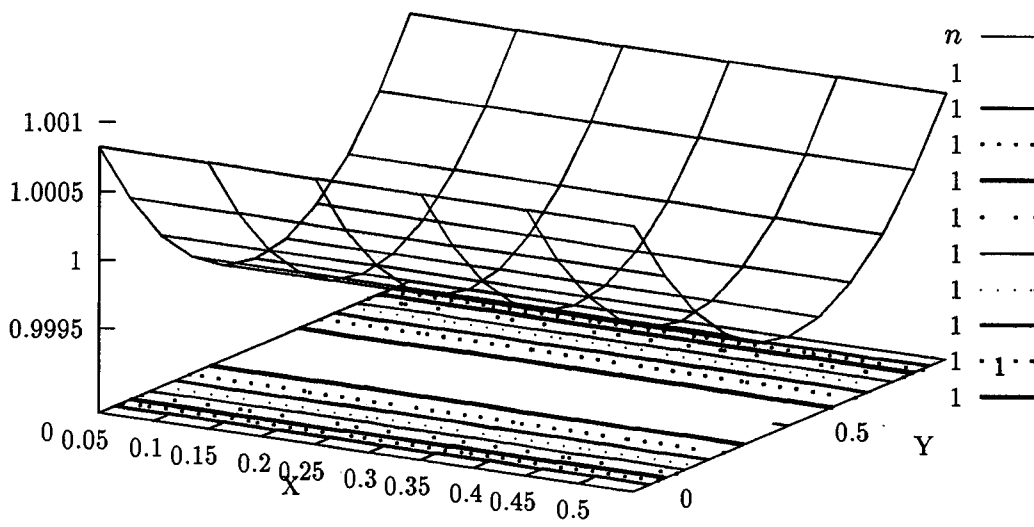


Figure 10: Density

## 6 Numerical Examples

The previous two sections compared kinetic simulations with an analytic solution and established confidence in the accuracy of the output. In this section, various Knudsen numbers are investigated in 1D2V and flow over an obstacle is investigated in 2D2V. All results are obtained with self-consistent values of density, mean molecular velocity, and temperature in the Maxwellian velocity-distribution function. As an added bonus, the 1D2V results were obtained on a variable structured mesh.

### 6.1 Various Knudsen Numbers

Extending the analysis of 1D2V plane Couette flow in the continuum regime, we examine a range of Knudsen numbers on a variable structured mesh. Results, obtained with full nonlinearity of the Maxwellian, are depicted in Figs. 11, 12, 13, and 14. As the Knudsen number increases, slip flow develops near the boundary. The analysis of this flow phenomenon was a topic focused on in the seminal papers referred to earlier in the paper.

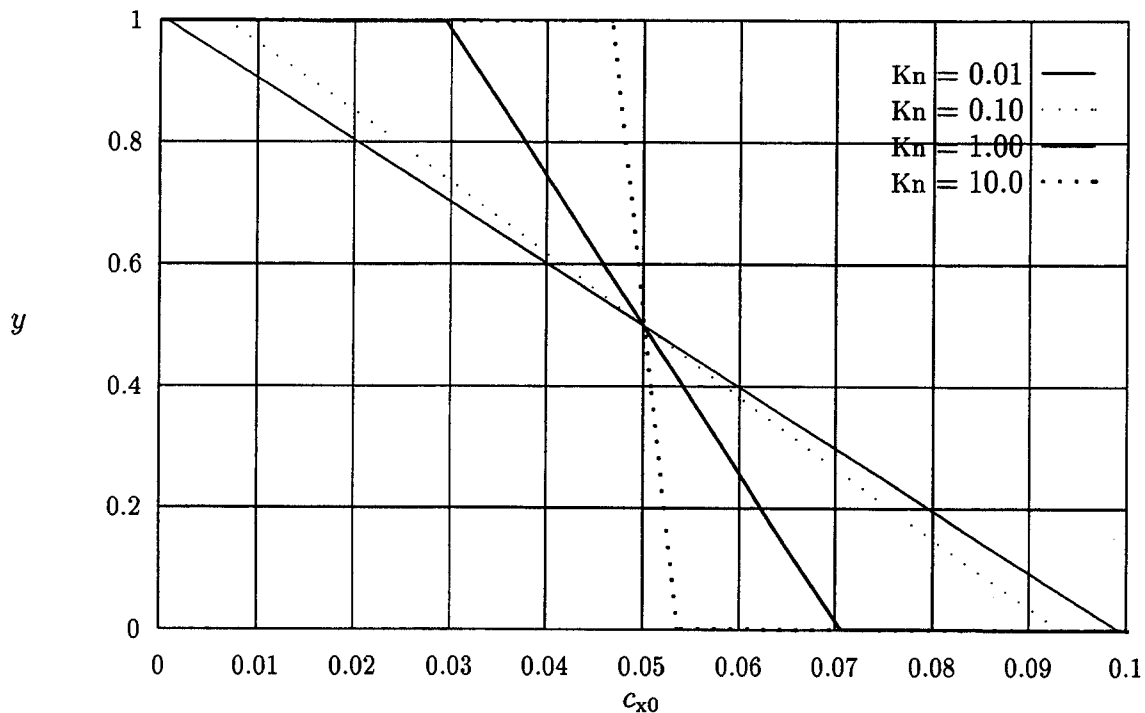


Figure 11: Mean Molecular Velocity in the  $x$ -Direction

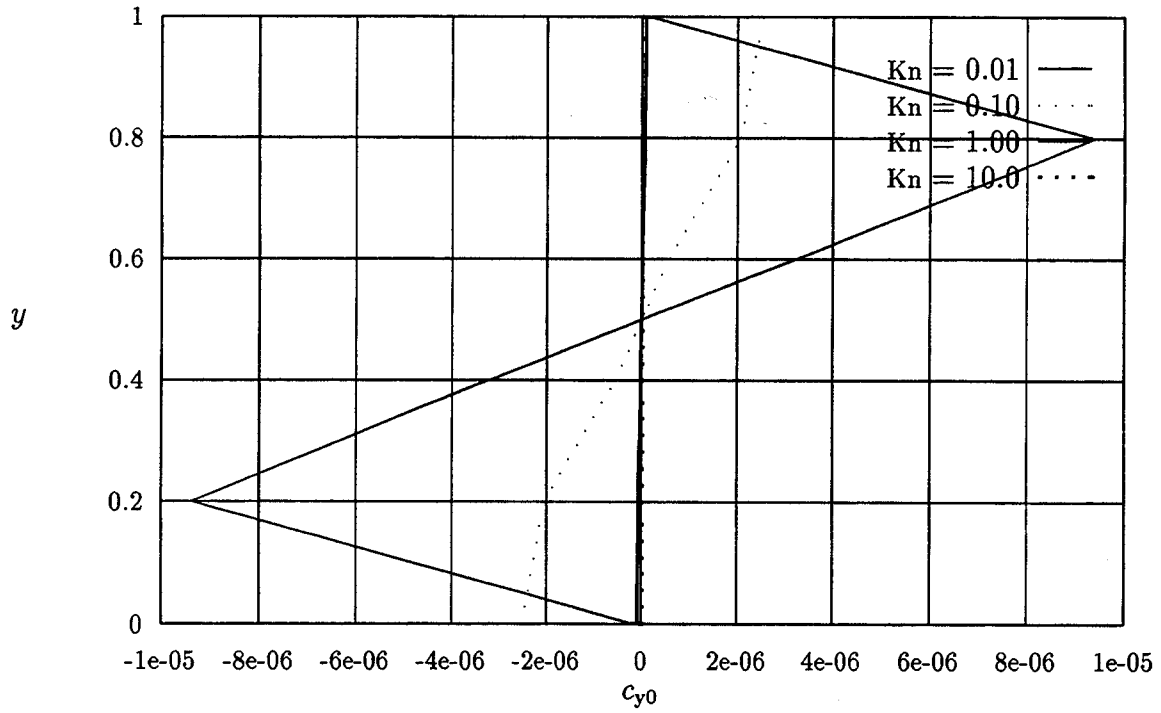


Figure 12: Mean Molecular Velocity in the  $y$ -Direction

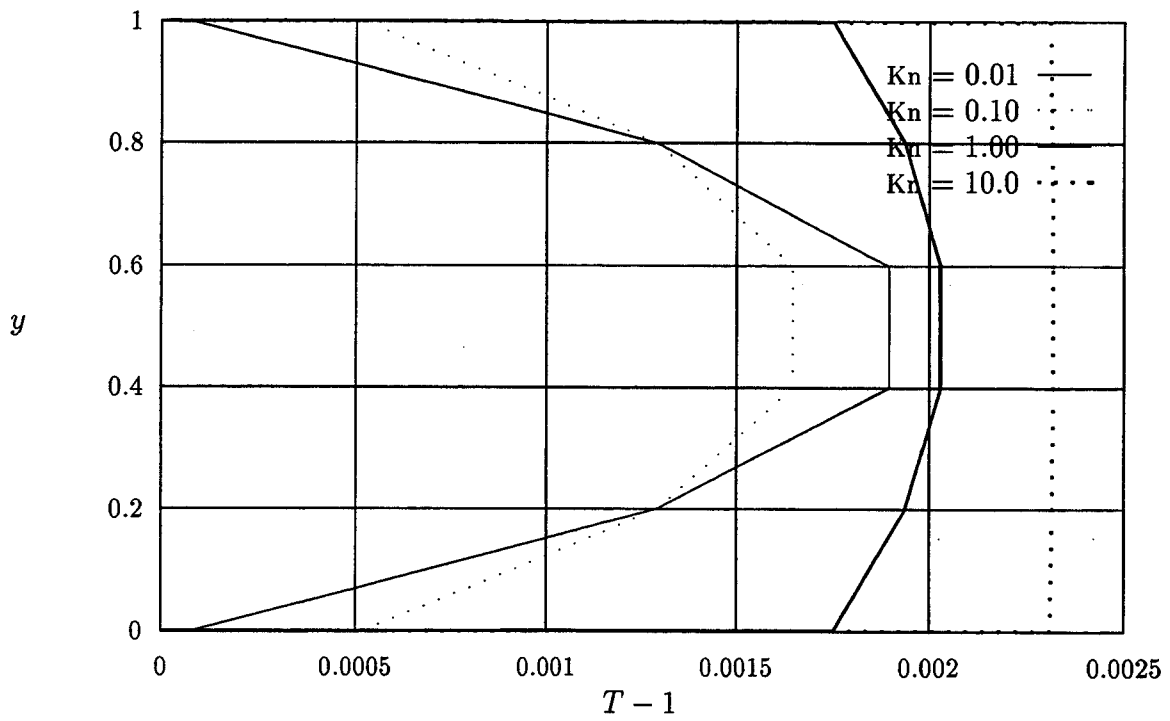


Figure 13: Temperature



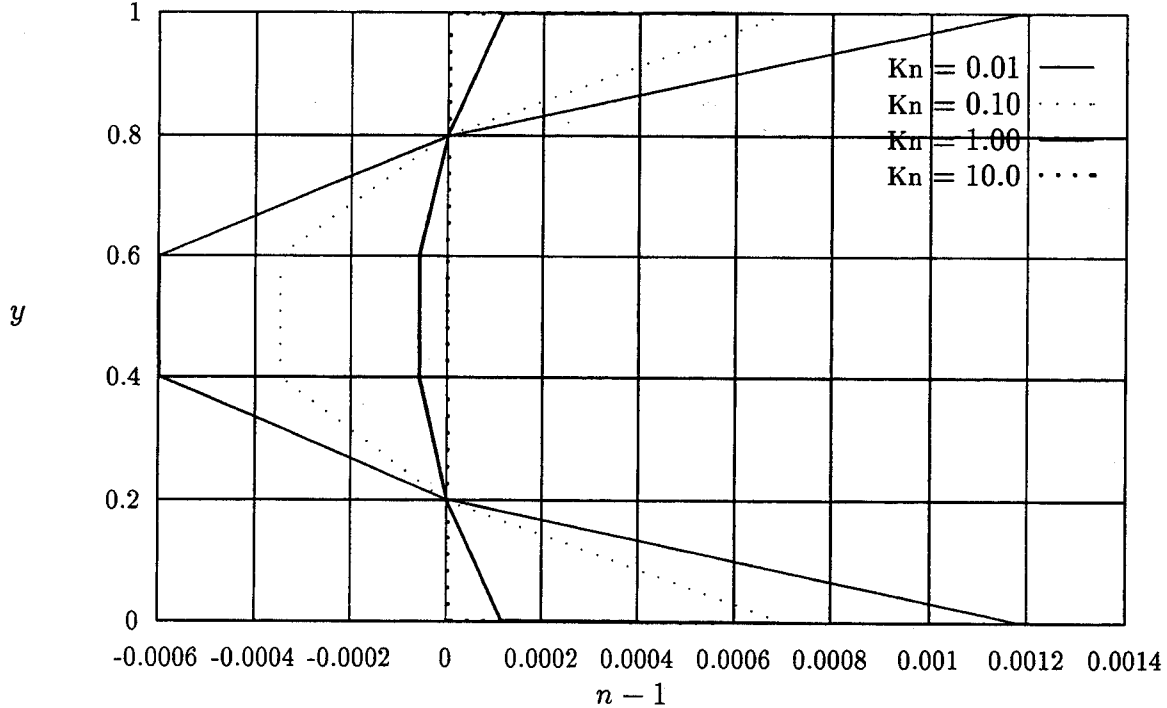


Figure 14: Density

## 6.2 Obstacle Flow

Extending the analysis of 2D2V plane Couette flow, performed in the continuum regime, we examine flow around an obstacle. Full nonlinearity of the Maxwellian is retained and a uniform structured mesh is used. Two flow regimes are depicted in the figures below. The first flow regime, depicted in Figs. 15-19, occurs when the distance between obstacles is small (hysteresis effects are unimportant in this study). The resulting flow pattern, commonly called a swirl, resembles a fluid within a cavity, acted on by a shearing stress. Increasing the distance between steps eventually allows for steady flow to develop and the formation of two eddies may be witnessed, see Figs. 20-22. Under the latter conditions we may estimate the connection length from the following interpolation formula given by Traub [12]:

$$\frac{d}{S} = -3.27 \cdot 10^{-6} \text{Re} + 0.0193 \text{Re} + 1.2, \quad (20)$$

where  $d$  is the connection length and  $S$  is the step height. With Reynolds number 5 and step height 0.5 this equation yields a value of 0.648 for the connection length, see Fig. 21. This value is consistent with our numerical simulations.

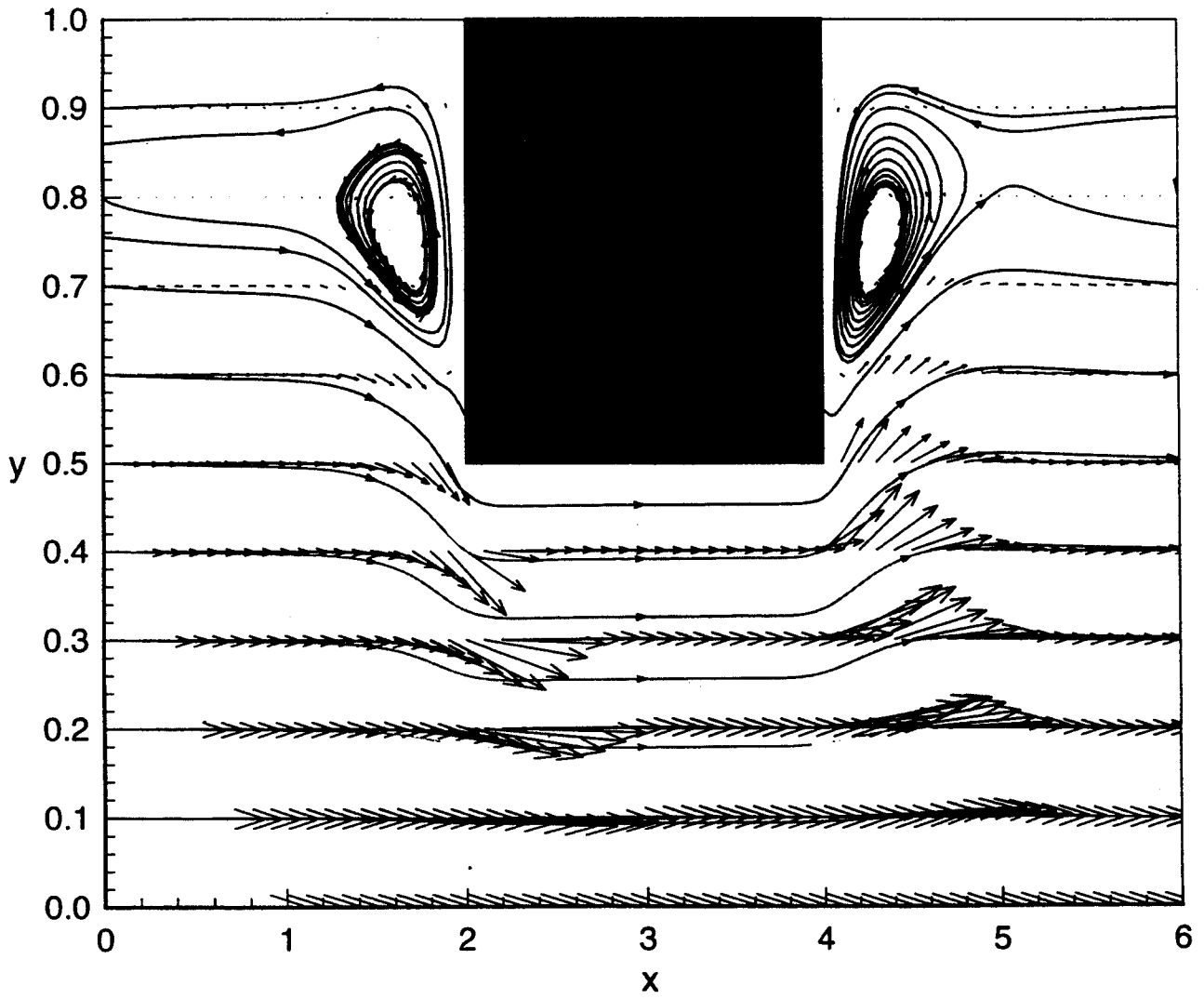


Figure 15: Mean Molecular Velocity (One Eddy)

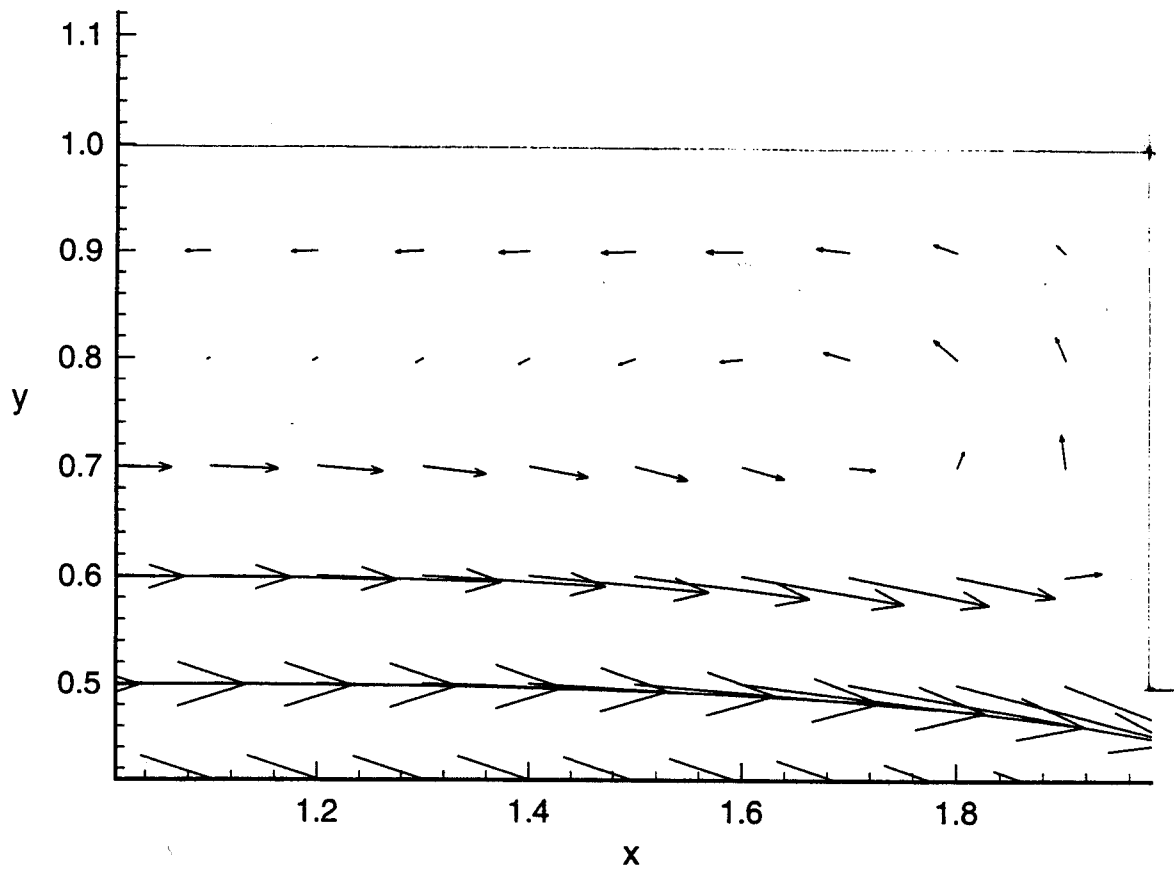


Figure 16: Mean Molecular Velocity in Front of Obstacle (One Eddy)

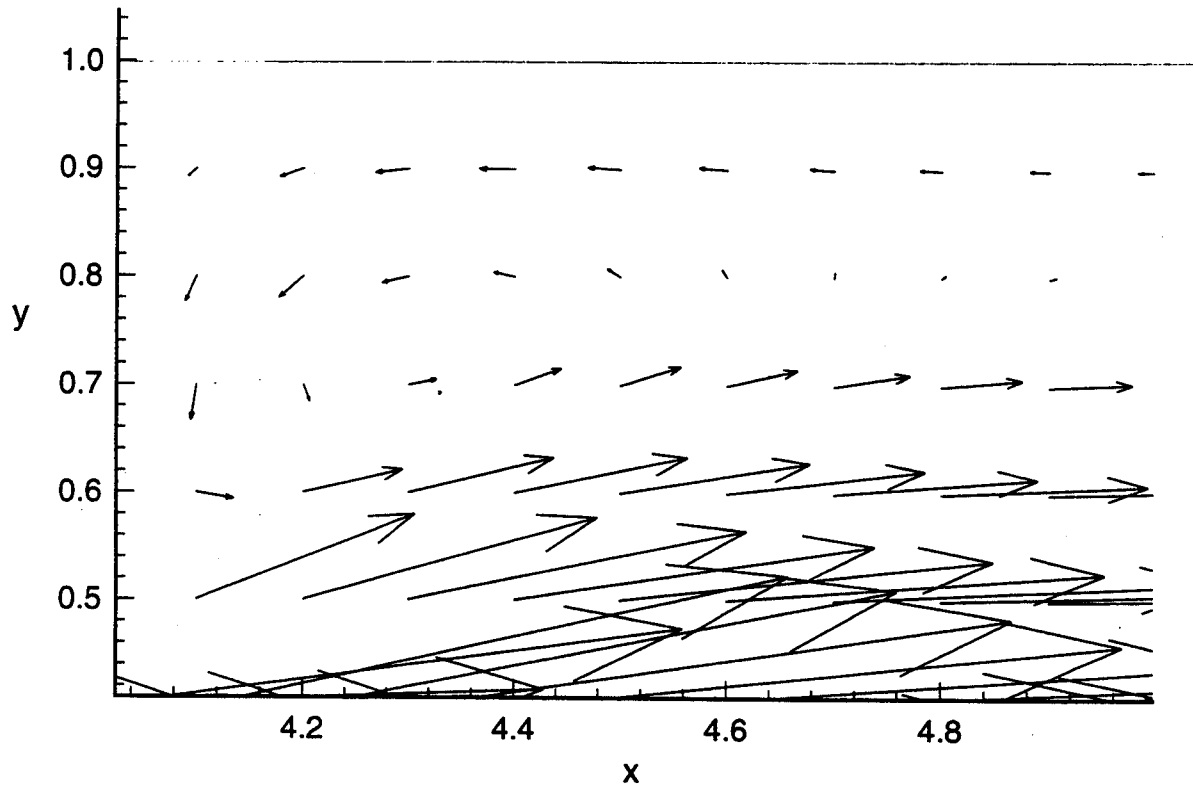


Figure 17: Mean Molecular Velocity in Back of Obstacle (One Eddy)

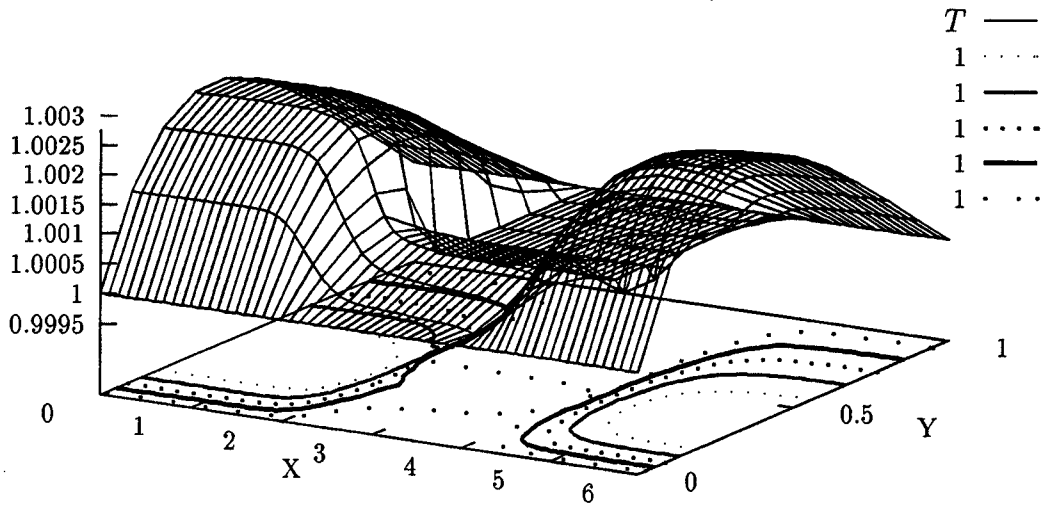


Figure 18: Temperature (One Eddy)

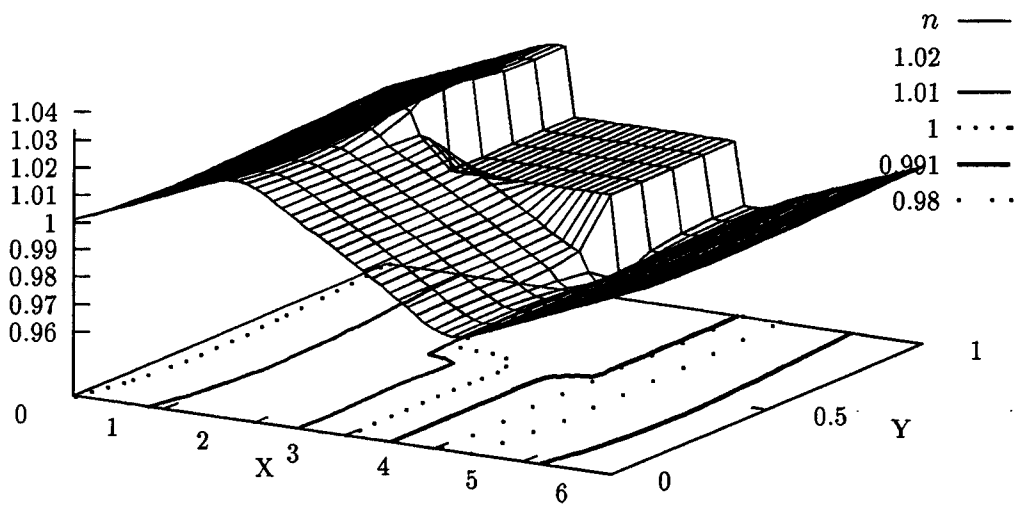


Figure 19: Density (One Eddy)

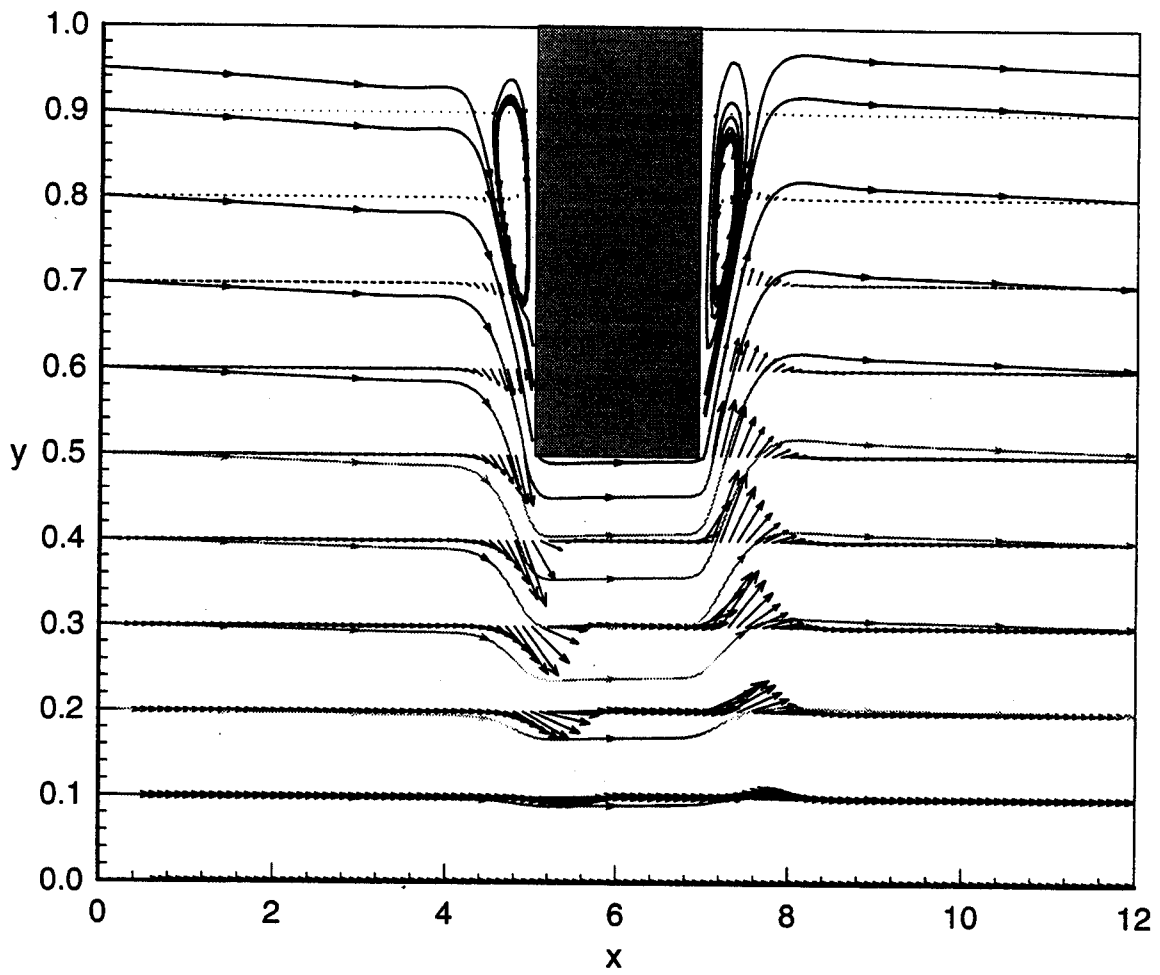


Figure 20: Mean Molecular Velocity (Two Eddies)

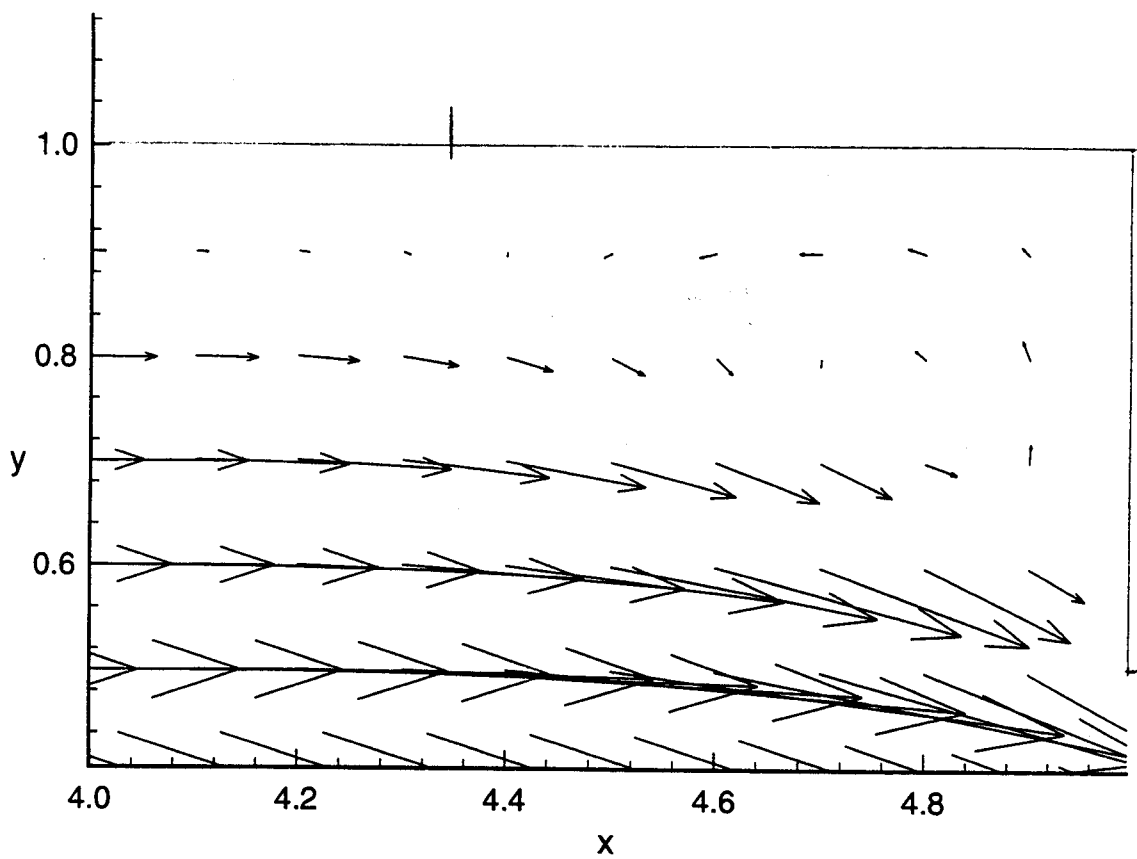


Figure 21: Mean Molecular Velocity in Front of Obstacle (Two Eddies)

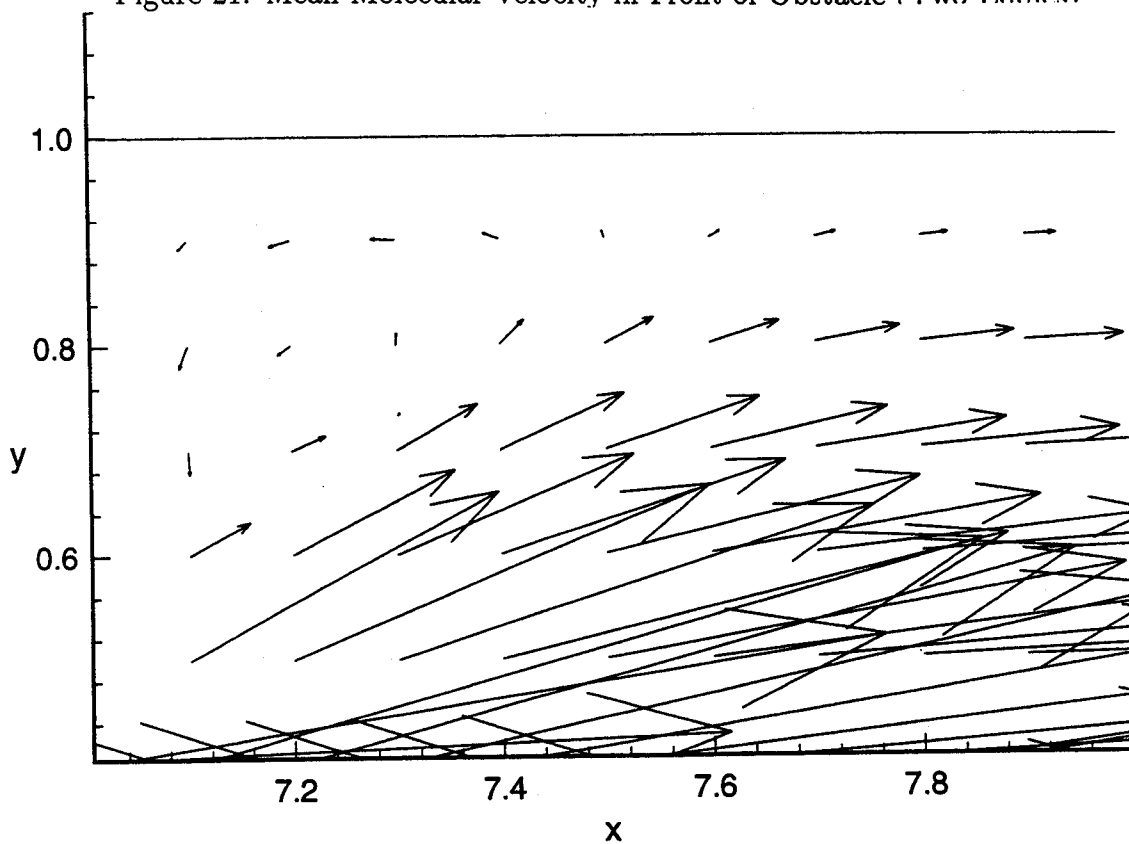


Figure 22: Mean Molecular Velocity in Back of Obstacle (Two Eddies)

## 7 Concluding Remarks

Formulation of an integral equation (using integration along characteristics of the general kinetic equation with Krook collision operator) and subsequent discretisation (with minimal complexity) was found to yield stable numerical solutions with mesh spacing much greater than the mean free path.

As the resulting integral equations are highly nonlinear, much is unknown about the behavior of this technique and any blind application of this technique is not warranted. In each simulation presented in this paper some feature of expected flow pattern was known; all simulations included an identical boundary condition that estimated the dynamics of flow patterns well but may not be suitable when energy transfer is important at the boundary. These issues deserve further attention and the authors hope a detailed error analysis is performed in the near future.

With independent space and time variables, integration along characteristic trajectories greatly enhances numerical efficiency (compared with traditional computational fluid dynamics (CFD) approaches such as the splitting technique or method of characteristics) and has the potential for massive parallelization. Since computational speed was not an issue in this paper no results were given, however we will mention that the one eddy obstacle simulation was performed on a Pentium 75 processor and required approximately 12.01 sec of CPU time per iteration and converged to machine accuracy after 5698 iterations. These topics warrant further numerical and computational analysis of the discretisation process used with this method.

## Acknowledgements

The authors appreciate the analytic guidance provided by Dieter J. Sigmar. MLA would like to thank his family for their support.

## References

- [1] P.C. Stangeby and G.M. McCracken. Plasma boundary phenomena in tokamaks. *Nuclear Fusion*, 30(7):1225, 1990.
- [2] D. Post, J. Abdallah, R.E.H. Clark, and N. Putvinskaya. Calculations of energy losses due to atomic processes in tokamaks with applications to the International Thermonuclear Experimental Reactor divertor. *The Physics of Plasmas*, 2(6):2328, 1995.
- [3] D.A. Knoll, P.R. McHugh, S.I. Krasheninnikov, and D.J. Sigmar. Simulation of dense recombining divertor plasmas with a Navier-Stokes neutral transport model. *The Physics of Plasmas*, 3(1):293, 1996.
- [4] E.M. Shakhov. *Method of Investigation of Rarefied Gas Motion*. Nauka, Moscow, 1974. [In Russian].
- [5] Carlo Cercignani. *Mathematical Methods in Kinetic Theory*. Plenum Press, New York, 2nd edition, 1990.
- [6] S. Chapman and T.G. Cowling. *The Mathematical Theory of Non-Uniform Gases*. Cambridge Mathematical Library Series 1990. Cambridge University Press, Cambridge, 3rd. edition, 1995.
- [7] Walter G. Vincenti and Charles H. Kruger Jr. *Introduction to Physical Gas Dynamics*. John Wiley and Sons, Inc., New York, 2nd edition, 1967.
- [8] E.P. Gross and S. Ziering. Kinetic theory of linear shear flow. *The Physics of Fluids*, 1(3):215, 1958.
- [9] E.P. Gross and E.A. Jackson. Kinetic models and the linearized Boltzmann equation. *The Physics of Fluids*, 2(4):432, 1959.
- [10] S. Ziering. Shear and heat flow for Maxwellian molecules. *The Physics of Fluids*, 3(4):503, 1960.
- [11] D.R. Willis. Comparison of kinetic theory analyses of linearized Couette flow. *The Physics of Fluids*, 5(2):127, 1962.
- [12] Kenneth R. Traub. Digital physics simulation of flow over a backward-facing step. [http://www.exa.com/DemosLow\\_Re\\_BFS.htm](http://www.exa.com/DemosLow_Re_BFS.htm), May 1994.